CONF-961113--3
ANL/TD/CP--91500

Contraband detection using high-energy gamma rays from $^{16}O^*$

Bradley J. Micklich, Charles L. Fink, Leonid Sagalovsky, and Donald L. Smith

Technology Development Division, Argonne National Laboratory
9700 South Cass Avenue, Argonne, IL 60439 USA

ABSTRACT

High-energy monoenergetic gamma rays (6.13 and 7.12 MeV) from the decay of excited states of the $^{16}O^*$ nucleus are highly penetrating and thus offer potential for non-intrusive inspection of loaded containers for narcotics, explosives, and other contraband items. These excited states can be produced by irradiation of water with 14-MeV neutrons from a DT neutron generator or through the $^{19}F(p,\alpha)^{16}O^*$ reaction. Resonances in $^{19}F(p,\alpha)^{16}O^*$ at proton energies between 340 keV and 2 MeV allow use of a low-energy accelerator to provide a compact, portable gamma source of reasonable intensity. The present work provides estimates of gamma source parameters and suggests how various types of contraband could be detected. Gamma rays can be used to perform transmission or emission radiography of containers or other objects. Through the use of (γ, n) and (γ, fission) reactions, this technique is also capable of detecting special nuclear materials such as deuterium, lithium, beryllium, uranium, and plutonium. Analytic and Monte Carlo techniques are used to model empty and loaded container inspection for accelerator-produced gamma, radioisotope, and x-ray sources.

Key Words: non-intrusive inspection, gamma rays, accelerators, contraband, nuclear materials

1. INTRODUCTION

Photons are widely used to perform non-intrusive interrogation of sealed containers. Typical applications are the examination of luggage and cargo containers for explosives or illicit substances (narcotics, weapons, etc.); radiographic examination of waste drums, structural components, etc.; and the detection of fissile materials and other heavy metallic objects. The qualities desired for the interrogating radiation are contrast (to be able to detect small anomalies) and penetration (to be able to see inside thick containers). A third desired quality, resolution, is primarily a function of the detectors used and the interrogation geometry. This paper discusses several photon sources currently used or proposed for non-intrusive inspection, including radioisotope sources (^{137}Cs and ^{60}Co), x-ray tubes (420 kV), electron linear accelerators (2.2 MV and 9 MV), and 6.13-MeV gamma rays from accelerator-produced $^{16}O^*$. Analytic and Monte Carlo models are used to compare these candidate sources.

2. PHOTON SOURCES

Photon sources currently used for non-intrusive container inspection are radioisotope sources such as ^{137}Cs (662 keV gamma energy) [1] and ^{60}Co (1.17 and 1.33 MeV), x-ray tubes operating at medium (420 kV) energies [2], or electron linear accelerators (e-linacs) using high (2 to 9 MV) accelerating potentials [3]. Photon sources from x-ray tubes or e-linacs produce a broad spectrum of photon energies, which makes deconvoluting the effects of photon scattering in large or dense objects extremely difficult. In addition, much of their intensity is in the low-energy portion of the spectrum, which usually adds to the dose delivered while contributing little useful information since it has low penetrability. Radioisotope sources can be used to obtain monoenergetic photons, but these are also limited by lower penetrability, source strength and the need for shielding when not in use.

Monoenergetic photons can also be created from the decay of nuclear excited states (gamma rays). For example, the first few excited states of the nucleus ^{16}O ($^{16}O^*$) decay by the prompt emission of 6.13- and 7.12-MeV gamma rays, producing a quasi-monoenergetic gamma source. These excited states can be created in several ways. One method is to use 14-MeV neutrons from a D-T neutron generator to activate water via the $^{16}O(n,p)^{16}N(\beta-)^{16}O^*$ process. The decay of 7.13-second ^{16}N radioactivity by $\beta-$ emission generates $^{16}O^*$ which, in turn, emits the 6.13- and 7.12-MeV gamma rays. The generated

DISCLAIMER

^{16}N activity can be transported to a remote location, well removed from the 14-MeV neutron source, where the interrogation procedures would be carried out. A second means of production uses proton bombardment of a thick target containing fluorine (e.g., calcium fluoride) at energies < 2 MeV (prominent resonances exist near 0.3, 0.7, 0.9 and 1.4 MeV, as well as an exponentially rising continuum beginning around 1.1 MeV) to induce the reaction $^{19}F(p,\alpha)^{16}O^*$. Both approaches are capable of generating strong portable 6.13-MeV gamma-ray sources. Depending upon the circumstances, one or the other approach for producing $^{16}O^*$ may be preferred. For example, the $^{19}F(p,\alpha)^{16}O^*$ process would yield essentially a point gamma-ray source. The alternative $^{16}O(n,p)^{16}N(\beta\text{-})^{16}O^*$ process lends itself to generation of an extended gamma-ray source or a source that can be transported inside an object.

The technology for 14-MeV neutron production using the D-T reaction is well established [4]. Compact and reliable neutron generators can be used to produce intense neutron radiation fields. Outputs of about 10^{11} neutrons per second into 4π steradians can be achieved routinely with commercially available machines. Neutron outputs that are one to two orders of magnitude greater have been generated with specially designed devices. It is estimated that a gamma-ray yield of about 0.02 gammas per D-T fusion neutron is feasible.

The $^{19}F(p,\alpha)^{16}O^*$ reaction has also been well studied, and thick-target gamma-ray yields have been widely measured for calcium fluoride targets [5,6]. Croft [7] reports a yield of $8.7 \cdot 10^7$/mA for the 340-keV resonance. The yield at the 940-keV resonance is at least an order of magnitude greater, and operation at 2 MeV incident energy would boost the yield by more than a factor of 100 [5]. Accelerators capable of producing proton beams of several milliamperes of current at 1-2 MeV are available commercially and are quite compact. The relative yield of 6.13- and 7.12-MeV gamma rays varies with the incident proton energy but the 6.13-MeV gamma ray is always dominant by a large margin. For example, the relative yields of gamma rays at the 340-keV proton resonance are: 6.13 MeV (97.0%), 6.92 MeV (0.3%) and 7.12 MeV (2.7%) [7]. Since the yield of 6.92-MeV gamma rays from the $^{19}F(p,\alpha)$ $^{16}O^*$ reaction is negligibly small by comparison with those for the 6.13- and 7.12-MeV gamma rays, this gamma ray is not considered further.

Characteristics of several photon sources used or proposed for container inspection are given in Table 1. While the electron linac sources are much stronger than the radioisotope or gamma sources, much of their output is in the form of low-energy photons. These photons are often completely absorbed in the interrogated object and contribute little or no information about the object's interior. By contrast, the 6.13-MeV gamma ray is highly penetrating, as shown by the lower attenuation coefficient in Figure 1. This means that a greater fraction of source photons will penetrate through thick objects, leading to lower dose delivered per amount of information obtained.

Table 1. Characteristics of photon sources used for non-intrusive inspection.

source	E or E_{ave} (MeV)	source strength (photons/Ci-s-cm^2 @ 1m or photons/mA-s-cm^2 @ 1m)	half life (yr)
^{137}Cs	0.662	$2.9 \cdot 10^5$	30.0
^{60}Co	1.17, 1.33	$5.9 \cdot 10^5$	5.27
$^{16}O(n,p)^{16}N(\beta\text{-})^{16}O^*$ (a)	6.13, 7.12	$1.6 \cdot 10^4$	
$^{19}F(p,\alpha)^{16}O^*$ (b)	6.13, 7.12	$6.9 \cdot 10^4$	
420-kV x-ray	0.114	$7.8 \cdot 10^9$	
420-kV x-ray (5 cm Al)	0.186	$7.0 \cdot 10^8$	
2.2-MV e-linac	0.62	$1.0 \cdot 10^{10}$	
2.2-MV e-linac (4 cm Fe)	0.99	$9.2 \cdot 10^8$	
9-MV e-linac	1.7	$1.2 \cdot 10^{12}$	
9-MV e-linac (6 cm Fe)	3.2	$1.0 \cdot 10^{10}$	

(a) For neutron generator producing 10^{11} n/s
(b) For incident proton energy of 2 MeV

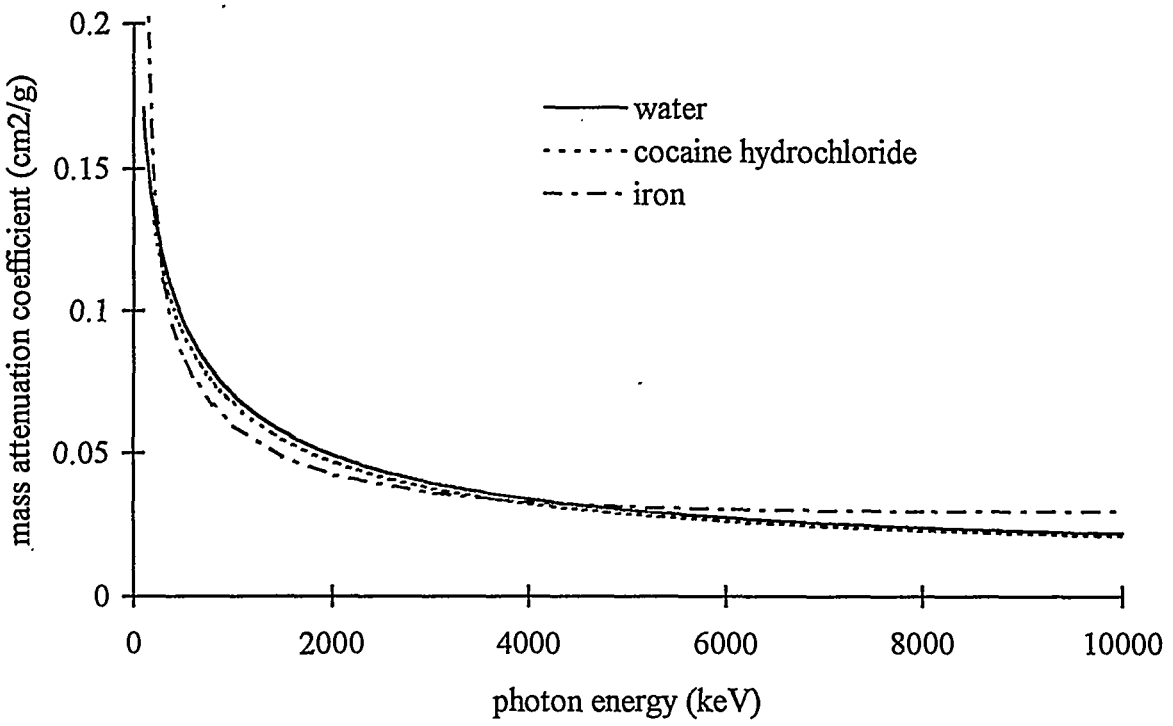

Figure 1. Photon mass attenuation coefficients for water, cocaine hydrochloride, and iron from 10 keV to 10 MeV.

Table 2 shows the results of calculations of source strengths required to obtain a count rate of 1000 counts per second in a 4-in NaI(Tl) detector located 10 m from the source. For each source, two simulated containers are considered. The first is an empty container or tank truck, represented by 5 cm iron. The second simulates a loaded container, for which the attenuation through 100 cm water is used. In addition, the radiation dose at one meter from the source is calculated using the source strength required to obtain the desired count rate of 1000/s. The source strengths are calculated using the equation

$$S \text{ (photons/sec)} \exp[-\mu t]\, \varepsilon\, A_d/4\pi r^2 = 1000 \text{ counts/sec}$$

where μ is the photon attenuation coefficient, t is the attenuator thickness, ε is the detector efficiency, A_d is the detector area, and r is the source-detector distance. For the continuum sources, the left side of the equation is generalized to include an integral over photon energy. This comparison gives an indication of the dose delivered by the source per unit of information obtained. In general, the x-ray and e-linac sources required small currents because of the sources' high yields, while the lower photon yield of the $^{19}F(p,\alpha)^{16}O^*$ reaction requires a larger current, on the order of several hundred microamperes. The 2.2- and 9-MV e-linacs deliver the lowest dose in the case of the thin absorber, with the dose from $^{19}F(p,\alpha)^{16}O^*$ being comparable to that from either ^{137}Cs or ^{60}Co. For the thick absorber (loaded container), the $^{19}F(p,\alpha)^{16}O^*$ and 9-MV e-linac sources deliver much smaller doses than any of the other sources, due to the more penetrating nature of their radiation. While the two sources are roughly equivalent in terms of inspection capability, the $^{19}F(p,\alpha)^{16}O^*$ source requires a more modest accelerator. Future work will address the question of shielding requirements for these sources.

Table 2. Photon source strength and radiation dose rate at 1 m for 1000 cps in 4-in NaI detector at 10 m.

attenuator	5 cm iron		100 cm water	
source	Ci/1000 cps or n/s/1000 cps or mA/1000 cps	dose rate @ 1 m from bare source (rad/hr)	Ci/1000 cps or n/s/1000 cps or mA/1000 cps	dose rate @ 1 m from bare source (rad/hr)
^{137}Cs	0.1	0.036	31	11.3
^{60}Co	0.035	0.043	2.5	3.1
$^{16}O(n,p)^{16}N(\beta-)^{16}O^*$	$4.4 \cdot 10^{10}$	0.044	$2.1 \cdot 10^{11}$	0.21
$^{19}F(p,\alpha)^{16}O^*$ (a)	0.1	0.044	0.48	0.21
420-kV x-ray (5 cm Al)	$4.6 \cdot 10^{-4}$	0.104	0.91	205
2.2-MV e-linac (4 cm Fe)	$1.36 \cdot 10^{-5}$	0.022	$8.55 \cdot 10^{-4}$	1.36
9-MV e-linac (6 cm Fe)	$5.76 \cdot 10^{-7}$	0.025	$5.1 \cdot 10^{-6}$	0.22

(a) For incident proton energy of 2 MeV

3. CONTRABAND DETECTION

Gamma rays from the decay of $^{16}O^*$ can be used for contraband detection in several ways. One interrogation technique is transmission or emission radiography. When the $^{16}O(n,p)^{16}N(\beta-)^{16}O^*$ source is employed, the generated ^{16}N activity can be transported to a location remote from the neutron field by pumping the water through a closed, circulating system which also allows for continuous regeneration of the source activity. In addition, the geometry can be tailored by the choice of shielding and the shape of the water conduit. Thus, either a collimated beam or a large area source can be created. Heavy metals and fissionable materials exhibit much higher absorption of photons than materials of lower atomic number and can be identified via radiography. Explosives and illicit drugs also tend to be more dense than the usual benign materials found in the luggage (e.g., clothing). A test of this concept has been performed [8]. The fact that the source can be transported in a small pipe also makes it useful for radiographing objects which are difficult if not impossible to access using a standard photon source. With this technique, the gamma source would be used much like conventional radioisotope or e-linac sources, except that its unique features (penetration, portability) make possible additional applications and operating scenarios.

A second interrogation technique, applicable only to fissionable material, exploits the fact that photofission cross sections for gamma rays with energies of 6-7 MeV are several millibarns in magnitude, while nearly all other elements have no photoneutron production at these photon energies (see Table 3). The Q-values (equivalent in magnitude to the neutron separation energy) shown in Table 3 were calculated using data from the Nuclear Wallet Cards [9]. Isotopic abundances are taken from the Chart of the Nuclides [10]. Indicated neutron energies are the maximum allowed by kinematics for the indicated gamma rays. The only elements and isotopes appearing in this table are those for which the (γ,n) thresholds are sufficiently low that neutron separation is energetically possible for at least the 7.12-MeV gamma ray. The light nuclides ^{2}H, ^{6}Li, and ^{9}Be are considered special nuclear materials (SNM) because of their roles in sensitive nuclear technologies associated with nuclear weaponry; they are treated as contraband materials in the present context. Clearly, only a relatively small number of (γ,n) reactions are energetically allowed over the periodic table for the dominant 6.13-MeV gamma ray, and these reactions result in low-energy neutrons. In comparison, (γ,f) reactions in fissionable materials yield neutrons which are more energetic, and therefore can be distinguished from those generated by (γ,n) reactions.

In this technique, the object to be interrogated is irradiated with the 6+-MeV gamma rays. Neutrons that are emitted from the induced photofission events are observed with a high-efficiency neutron detector which incorporates gamma-ray discrimination. For this application, the $^{19}F(p,\alpha)^{16}O^*$ process might be more favorable because no neutrons are generated by this reaction at the low proton energies involved. Preliminary calculations concerning the neutron source intensity and geometry for a luggage or small container inspection system indicate that one would observe 10-20 counts per second due

Table 3. Calculated (γ,n) Q-values and neutron energies.

	Target	Isotopic		Neutron Energy (MeV)	
Element	Isotope	Abundance (%)	Q-Value (MeV)	6.13-MeV γ	7.12-MeV γ
Light Elements					
Hydrogen	^{2}H	0.015	-2.225	3.904	4.890
Lithium	^{6}Li	7.5	-5.660	0.469	1.455
Beryllium	^{9}Be	100	-1.665	4.464	5.450
Carbon	^{13}C	1.11	-4.946	1.183	2.169
Oxygen	^{17}O	0.038	-4.143	1.986	2.972
Neon	^{21}Ne	0.27	-6.761	-	0.354
Medium Elements					
Zinc	^{67}Zn	4.1	-7.052	-	0.063
Germanium	^{73}Ge	7.73	-6.783	-	0.332
Molybdenum	^{97}Mo	9.55	-6.821	-	0.294
Ruthenium	^{101}Ru	17.0	-6.802	-	0.313
Palladium	^{105}Pd	22.33	-7.094	-	0.021
Heavy Elements [a]					
Tin	^{117}Sn	7.68	-6.945	-	0.170
	^{119}Sn	8.58	-6.485	-	0.630
Tantalum	^{180}Ta	0.12	-6.645	-	0.470
Tungsten	^{183}W	14.3	-6.191	-	0.924
Platinum	^{195}Pt	33.8	-6.105	0.024	1.010
Lead	^{207}Pb	22.1	-6.738	-	0.377

[a] Other heavy elements for which the (γ,n) reaction is energetically possible, but which are unlikely to be present in ordinary luggage and cargo containers, are Cd, Te, Xe, Ba, Nd, Sm, Gd, Dy, Er, Yb, Lu, Hf, Os, and Hg.

to fission neutrons for 1 kilogram of fissionable material. Measurements have also shown that photofission occurred when a fission detector containing depleted uranium (^{238}U) was placed in the vicinity of radioactive water generated using an intense neutron generator [11]. Under appropriate conditions, radiography and photofission can be performed simultaneously, permitting the user to image fissile materials hidden in large containers.

4. MONTE CARLO STUDIES

The Monte Carlo radiation transport code MCNP [12] was used to perform simulations of detector response for container interrogation using the photon sources described above. Two simple container models were used. In the first (Figure 2), an empty tanker was assumed to have cocaine hidden inside in the form of a thin (5 or 10 cm) layer attached to the side. This model provides an indication of the contrast available using the various photon sources. In the second model (Figure 3), a larger amount of cocaine (50 cm thick) was assumed to be hidden inside a tanker filled with water. This model provides an indication of the penetrability of the various radiation sources.

Figure 4 shows the counts per source photon for the radioisotope and gamma-ray sources. For these monoenergetic sources, the detectors are assumed to operate in a pulse-counting mode with an energy threshold, since this would allow scattering corrections to be made. For the ^{137}Cs and ^{60}Co sources, the full-energy peaks are counted, while for the 6.13-MeV gamma source all events with energy equal or higher than that of the double escape peak are counted. All sources provide enough contrast to see the location of the hidden cocaine. The greater penetrability of the 6.13-MeV gamma source is also clearly seen by the greater number of photons penetrating the tank walls. Figure 5 shows the simulation results for the 420-kV x-ray and the 2.2-MV and 9-MV electron linac sources. For these continuum sources, all photons were counted, although in practice one would employ some energy threshold sufficient to screen out low-energy noise pulses. The signal to background ratio for the six sources considered can be estimated as 1-(C1/C2), where C1 is the count rate in the detectors behind the cocaine and C2 is the count rate in the

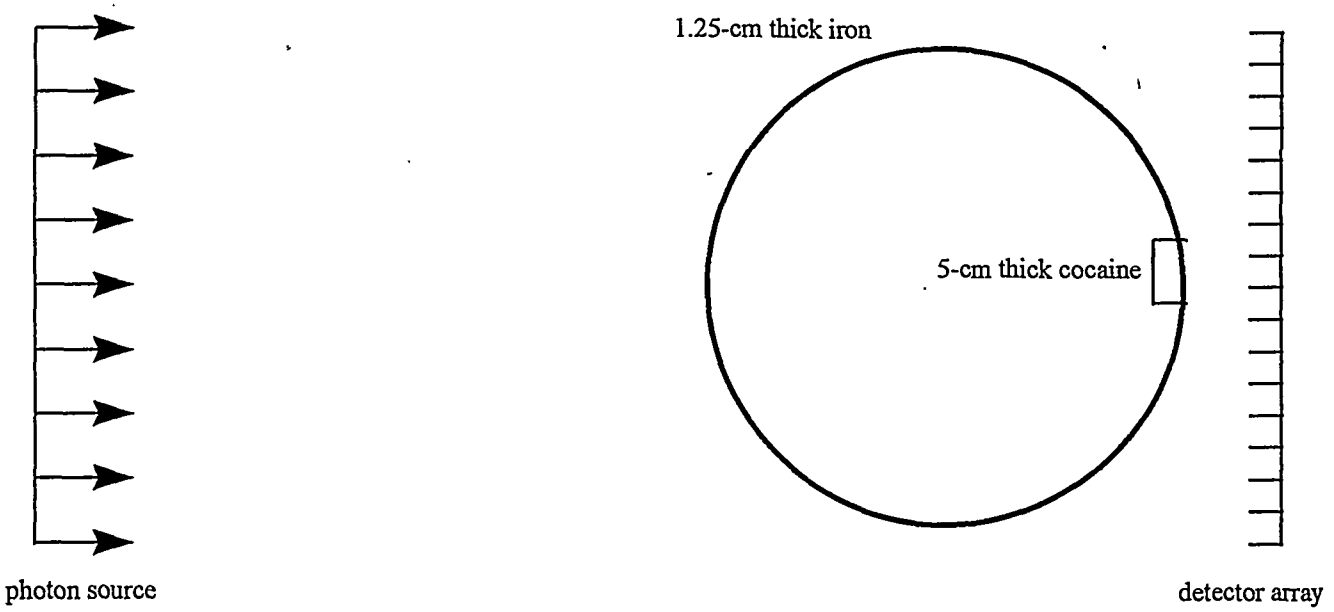

Figure 2. Empty tanker model for MCNP photon interrogation simulations.

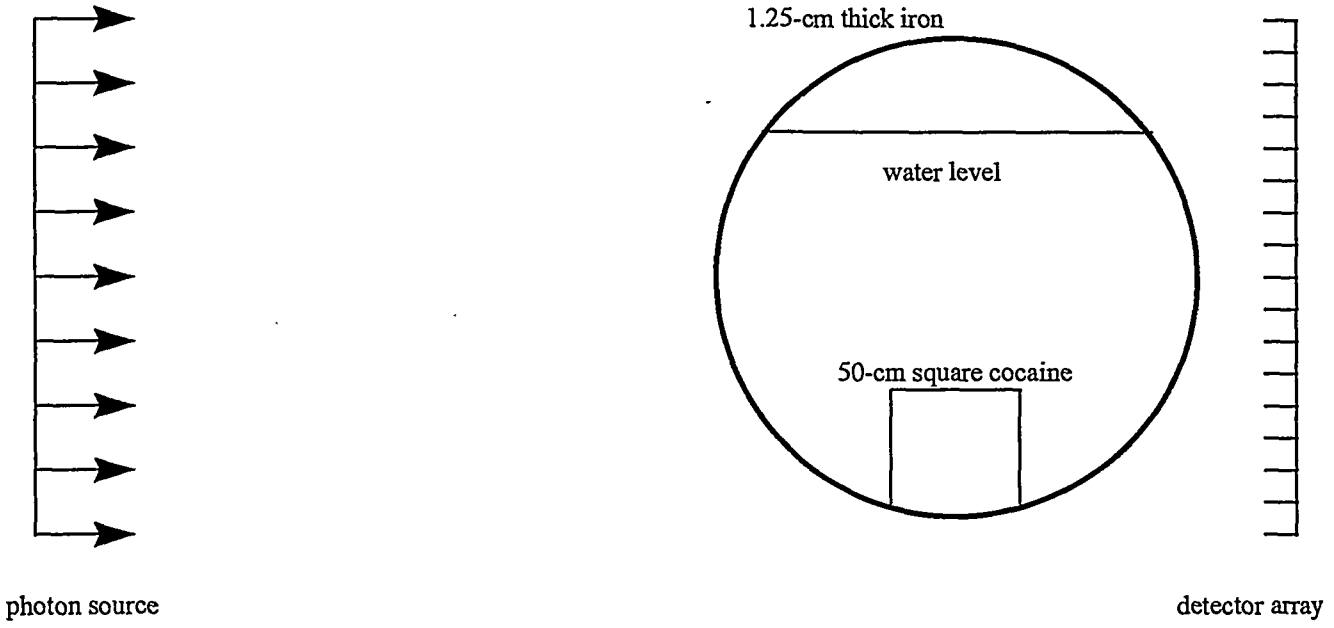

Figure 3. Water-filled tanker model for MCNP photon interrogation simulations.

detectors immediately to either side. On this basis, the 420-kV x-ray and ^{137}Cs radioisotope sources give roughly the same results: S/B of 63% for the 420-kV x-ray source and 60% for the ^{137}Cs source. As expected, the S/B is worst for the highest energy sources: 31% for the 9-MV e-linac and 27% for the 6.13-MeV gamma source. The signal to background for ^{60}Co 50%) and the 2.2-MV e-linac (43%) lie in between.

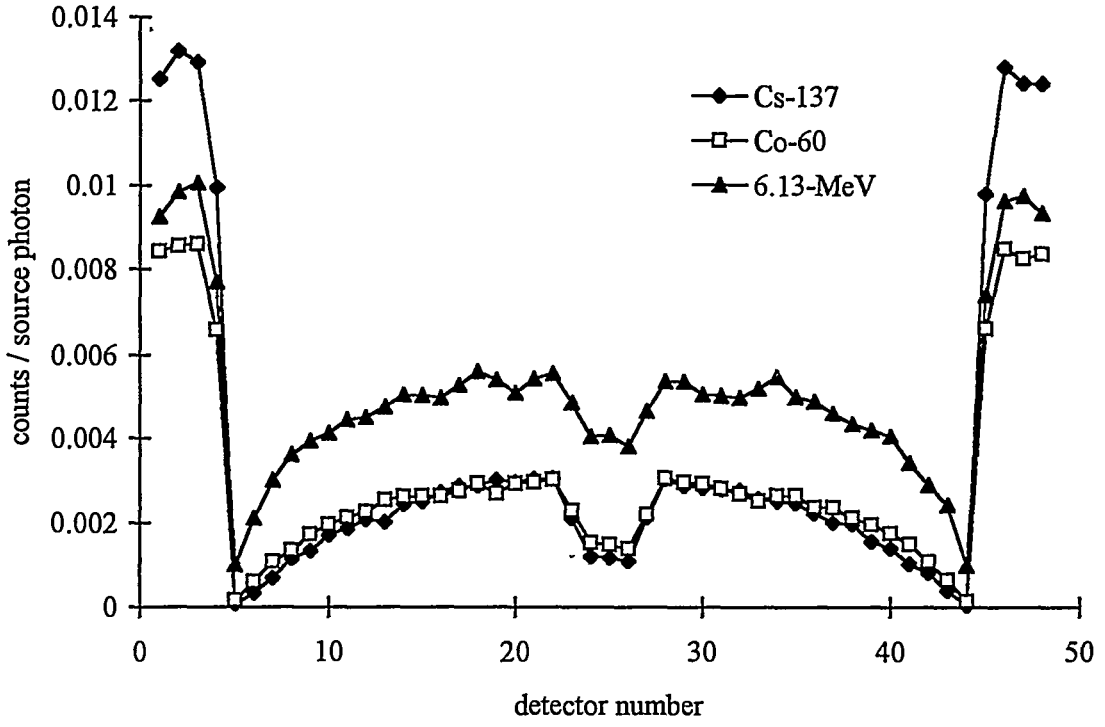

Figure 4. Counts per source photon vs. detector for 5 cm cocaine hydrochloride hidden inside empty iron tank.

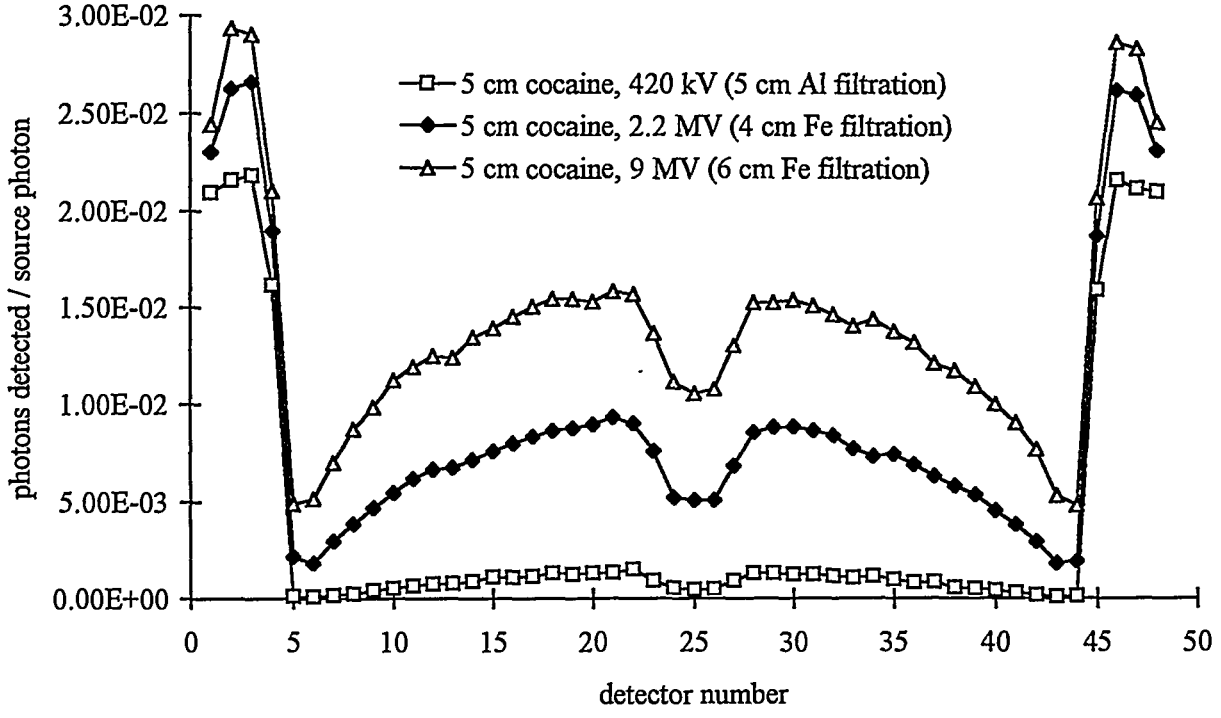

Figure 5. Counts per source photon vs. detector for 5 cm cocaine hydrochloride hidden inside empty iron tank.

The simulation results for the water-filled tanker with the 50-cm thick cocaine are shown in Figure 6 for both the 6.13-MeV gamma and the 9-MV e-linac sources. Simulations were not performed for the other sources because the transmissions would be too low to be of practical use. For both sources, the count rate behind the hidden cocaine is about 18% lower than in the case of the tank containing water only. Count rates through the water in the tank are the same for the two sources, while the count rates due to the 9-MV source are higher for paths through the air because of the higher average detector efficiency. There is an increase in counts for detectors just below the water/air interface in the case of the 9-MV e-linac which is not present for the 6.13-MeV gamma source. This is due to scattered photons, which are not counted in the case of the monoenergetic 6.13-MeV source because of the threshold employed. A similar threshold could be used for the 9-MV e-linac, but at a cost of reduction in count rate. This is one example of the type of scattering corrections possible when the source is monoenergetic.

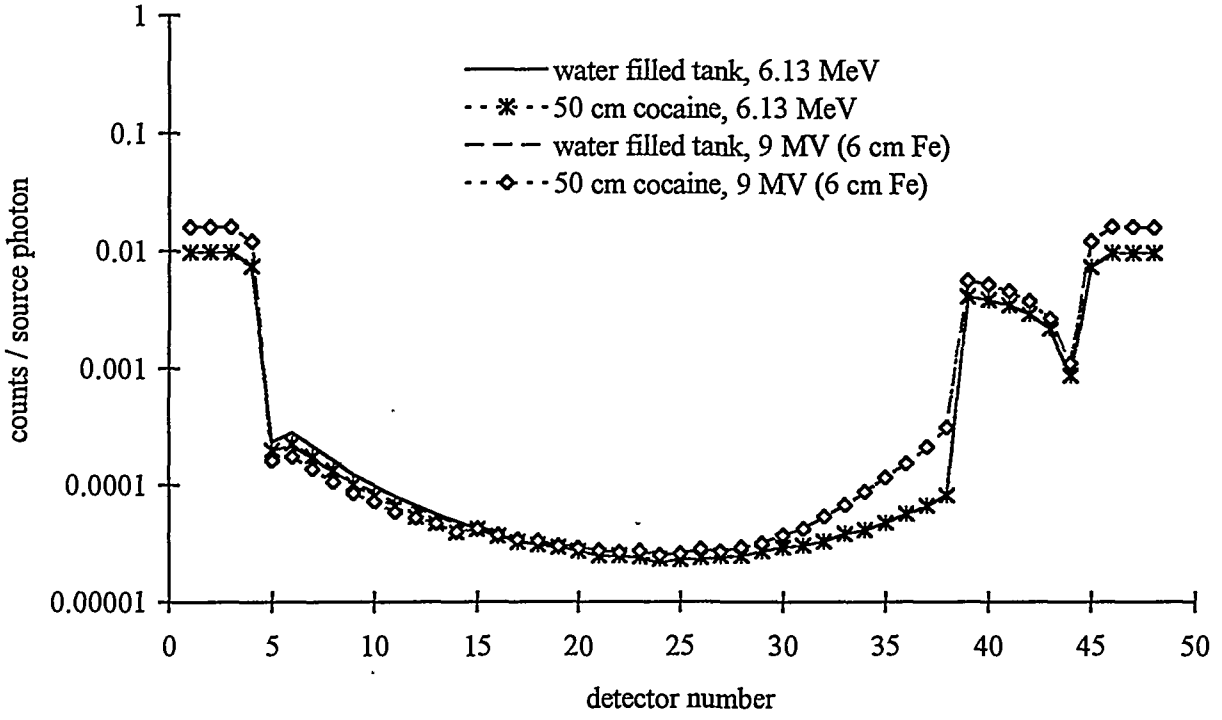

Figure 6. Counts per source photon vs. detector for 50-cm cocaine cube hidden inside water-filled tanker.

5. CONCLUSIONS

The 6.13- and 7.12-MeV gamma rays from $^{16}O^*$ provide an attractive alternative to the lower-energy gamma rays from ^{137}Cs and ^{60}Co. The higher energy allows interrogation of dense or thick objects which cannot be penetrated by the lower energy gamma rays. For less dense or thinner objects, the signal to background ratio is somewhat but not significantly better for the radioisotope sources. The $^{16}O^*$ gamma source also has a lower dose rate. The ability to turn the source of gamma rays on and off with the accelerator should provide a decrease in the radiological controls required to operate the source. The actual costs of the radioisotope sources would probably be lower than for the $^{16}O^*$ source. Future efforts will examine system issues such as size and costs.

A comparison between the $^{16}O^*$ gamma source and e-linacs indicates that they will have similar penetrability and S/B ratios. The e-linac will always have a higher dose that the monoenergetic source due to the broad spectrum of

x-ray energies. The monoenergetic source will have fewer scattering artifacts. A key advantage of the e-linacs is the high photon yield from the source. The costs and sizes of comparable systems will be objects of future study.

Finally, the $^{16}O^*$ gamma source could provide a simple, effective method of detecting contraband nuclear materials, although more work is needed to define system parameters.

6. ACKNOWLEDGMENTS

This work was sponsored by the Office of National Drug Control Policy, Counterdrug Technology Assessment Center, under contract number TV-94591V.

7. REFERENCES

1. V. V. Verbinski, "Cargo vehicle inspection system," Proc. Int'l technology Symposium on Counterdrug Law Enforcement," Nashua, NH (Oct. 1995).
2. R. D. Swift and R. P. Lindquist, "Medium energy x-ray examination of commercial trucks," SPIE **2276**, 242-254 (1994).
3. R. W. Volberding and S. M. Khan, "Cargo container inspection test program at ARPA's Nonintrusive Inspection Technology testbed," SPIE **2276**, 210-217 (1994).
4. P. Bach, M. Jatteau, J. L. Ma, C. Lambermont, "Industrial analysis possibilities using long-life sealed-tube neutron generators," *Journal of Radioanalytical and Nuclear Chemistry*, **168**, No. 2, 393-401 (1993).
5. S. O. F. Dabaneh, K. Toukan, and I. Khubeis, "Excitation function of the nuclear reaction $^{19}F(p,\alpha\gamma)^{16}O$ in the proton range 0.3-3.0 MeV," *Nucl. Instr. Meth. Phys. Res.* **B83**, 319-324 (1993).
6. D. Dieumgard, B. Maurel, and G. Amsel, "Microanalysis of fluorine by nuclear reactions I. $^{19}F(p,\alpha_0)^{16}O$ and $^{19}F(p,\alpha\gamma)^{16}O$ reactions, Nucl. Instr. Meth. **168**, 93-103 (1980).
7. S. Croft, "The Absolute Yield, Angular Distribution, and Resonance Widths of the 6.13, 6.92, and 7.12 MeV Photons from the 340.5 keV Resonance of the $^{19}F(p,\alpha_0)^{16}O$ Reaction," *Nucl. Instr. Meth. Phys. Res.* **A307**, 353-358 (1991).
8. D. L. Smith, Y. Ikeda, and Y. Uno, "An investigation into the possibility of performing radiography with gamma rays emitted from water made radioactive by irradiation with 14 MeV D-T fusion neutrons," *Fus. Eng. Des.* **31**, 41-52 (1996).
9. J. Tulli, "Nuclear Wallet Cards," National Nuclear Data Center, Brookhaven National Laboratory (1995).
10. F. W. Walker, J. R. Parrington, and F. Feiner, "Nuclides and Isotopes, 14th ed." G. E. Nuclear Energy (1989).
11. D. L. Smith, F. Maekawa, and Y. Ikeda, "Observation of Photofission Induced by Gamma Rays from the Decay of ^{16}N Generated in Water by D-T Fusion Neutrons," manuscript in preparation.
12. J. Briesemeister, ed., "MCNP - A General Monte Carlo N-Particle Transport Code, Version 4A," LA-12625-M, Los Alamos National Laboratory (Nov. 1993).